Paper No. 820. (quote when citing this article)
Eleventh World Conference on Earthquake Engineering
ISBN: 0 08 042822 3

THE DUCTILITY OF CARBON FIBRE REINFORCED CONCRETE JOINTS IN SEISMIC AREAS

G.ZINGONE, L.LA MENDOLA and G.CAMPIONE

Dipartimento di Ingegneria Strutturale e Geotecnica,
Università di Palermo, Viale delle Scienze, I90128, ITALY

ABSTRACT

The collapse of framed reinforced concrete buildings under high seismic actions is often due to brittle failure of the beam-column joints because of the inadequate ductility available. Better behaviour of the joints can be obtained by inserting a large amount of transverse reinforcements, but their arrangement is often very problematic. In order to overcome this drawback a simplified arrangement of the transverse reinforcements can be integrated by the use of fibre reinforced concrete. In the present paper the behaviour of the carbon fibre reinforced concrete (CFRC) is analysed because it offers more advantages then other fibres types.

In the case in which the joint is overstrong with respect to beams and columns convergent in it, and the columns are overstrong with respect to the beams too, failure occurs in the beam-column cross-sections. Hence the analysis of the cyclic behaviour must be carried out with reference to the cross-sections above, in terms of moment-curvature diagrams. This implies knowledge of the constitutive laws in compression and in tension of the materials (CFRC and longitudinal steel reinforcement).

By an experimental program, based on monotonic and cyclic tests, the behaviour of the CFRC with and without transverse reinforcement is analysed, considering different percentages of fibres. Finally, an analytic law that fits in with good approximation with the experimental results is proposed. Then the cyclic behaviour of rectangular cross-sections in CFRC and longitudinal steel reinforcement under bending moment and axial force is analysed, in order to evaluate the improvement due to the presence of the fibres in the concrete.

KEYWORDS

Carbon fibres; reinforced concrete; experimental tests; stress-strain laws; cyclic behaviour; flexural ductility.

INTRODUCTION

In the regions of the joints (beam-column joints, fixed bases of the shear walls, etc.) of concrete structures in seismic areas, to withstand the shear forces and the bending moments induced by repeated cyclic actions, large amounts of longitudinal and transverse reinforcement are required. To simplify the fabrication of such joints the use of CFRC in these regions, partially substituting the transverse reinforcement, is proposed. This type of fibre in concrete is particularly suitable with respect to other types (steel, glass, synthetic fibres, etc.), because of high mechanical properties, low weight density, etc.

The use of CFRC is particularly recommended when, under the cyclic action due to an earthquake, the damage appears in the joint with typical shear cracks. In these cases, if the joint is not adequately confined by transverse reinforcement, the failure is brittle, and it is caused by the fact that the tensile strength of the concrete is exceeded (Katzensteiner *et al.*,1994). If CFRC is used, there is an improvement in the dissipative capacity of the plastic hinges, localised at the cross-sections (in the plastic-hinge region the failure mode of a beam from flexural-shear failure to flexural failure can change as said in Jiuru *et al.*,1992). This improvement is linked to the high deformation capacity in compression of CFRC with low reduction of stress that is obtained by using a high percentage of fibres (Zingone *et al.*, 1995).

The advantages of using fibres consist in: - bridging across cracks in the concrete; - restricting the width and extension of cracks; - increasing the shear resistance of the joints. The resistance of the joints is connected to the tensile strength of CRFC, higher than the tensile strength of plain concrete, particularly in the post-cracking phase (Jiuru *et al.*, 1992).

The present study relates to CFRC behaviour with and without transverse reinforcement. Experimental results are utilised to study the cyclic behaviour of CFRC cross-sections with longitudinal bars under cyclic actions (bending moments and axial forces). It is important to analyse the behaviour of the plastic hinges that occur at the beam cross-sections adjacent to the columns and at the fixed ends of the columns in the global mechanism collapse in framed buildings in seismic areas.

BEHAVIOUR OF PLAIN AND FIBRE REINFORCED CONCRETE JOINTS

In an earthquake resistant reinforced concrete frame the joints are generally considered rigid. Under the cyclic actions induced by an earthquake, the core of the joint is subjected to several shear forces. The tensile and compressive stresses that arise are supported in a joint of plain concrete by the longitudinal and transverse steel reinforcements; in a joint of CFRC with ordinary reinforcements a strong contribution to shear resistance is made by the tensile strength of the carbon fibre concrete. Insufficient anchorage and degradation of the bond in slip always cause the premature failure of the joint, producing the slippage of the longitudinal bars with lost of strength and ductility capacity. In these cases the use of the CFRC is suitable (Bentur and Mindess, 1990; Olariu *et al.*,1988; Jiuru *et al.*, 1992; Katzensteiner *et al.*,1994; Filiatrault *et al.*, 1994).

Several codes propose to assign overstrength to the core of the joints with respect to the beams and columns in the framed structures. In these cases the dissipative mechanism is localised in cross-sections between beams and columns. Recent studies show that the use of fibres homogeneously distributed in the matrix (plain concrete) in an appropriate percentage performs the same function as transverse reinforcement and increases the tensile strength of the matrix, reducing cracking under cyclic loading.

The behaviour of the joint in CFRC without transverse reinforcement is thus explained: as soon as the value of the tensile stress attains the tensile resistance peak, first-cracking appears and a loss of strength is noted; if the load increases failure occurs if the post-cracking tensile strength is exceeded. In these cases fibre pull-out occurs. Regarding these aspects it is very important to determine the values of the first-cracking and post-cracking tensile strength with an experimental program based on tensile tests.

EXPERIMENTAL SCHEME : MATERIALS AND MIX PROPORTIONS

The carbon fibre concrete consisted of Portland cement in a percentage, according to the maximum aggregate size used, equal to 400 Kg/m^3. The maximum aggregate size, related to the fibre length utilised (L_f=20 *mm*), was 15 *mm*. The percentages of the aggregate used were the following: sand 8%, crushed stone 33% and basalt (5-15 *mm*) 58%, its weight density is 1800 Kg/m^3. The water-cement ratio was 0.41; superplasticizers in a percentage between 1% and 1.5%, to maintain good workability and related to the fibre percentage available were used. The fibres utilised are obtained by carbon with an opportune process, reducing the characteristic fragility; the equivalent diameter is ϕ=0.78 *mm*. The addition of fibres homogeneously mixed in the matrix was in the following volume percentage V_f: 0.38%, 1.52%, 3.04% (4, 16, 32 Kg/m^3).

A series of cylindrical specimens were fabricated for the experimental program consisting in a series of monotonic and cyclic compressive and monotonic tensile tests. The size of these cylindrical specimens was: diameter 10 *cm*, height 20 *cm*. The series fabricated were the following: plain concrete; concrete with transverse reinforcement; carbon fibre concrete; carbon fibre concrete with transverse reinforcement. The transverse reinforcement, consisting in spirals with an outer diameter of 7 *cm*, was fabricated by using steel bars having diameter equal to 6 *mm* and yielding stress f_{yk} =380 *MPa*.

MONOTONIC COMPRESSIVE LOADING

A series of cylindrical specimens under monotonic compressive loading were tested. Tests were carried out in a closed-loop servocontrolled testing machine. The deformations were measured over the entire length of the specimen and the constant rate of platen-to-platen displacement corresponded to a strain rate of 2 *μm/sec*. The results of tests on plain concrete and carbon fibre reinforced concrete are plotted in Fig. 1, where the parameter of the curves is $RI=V_f L_f/\phi$.

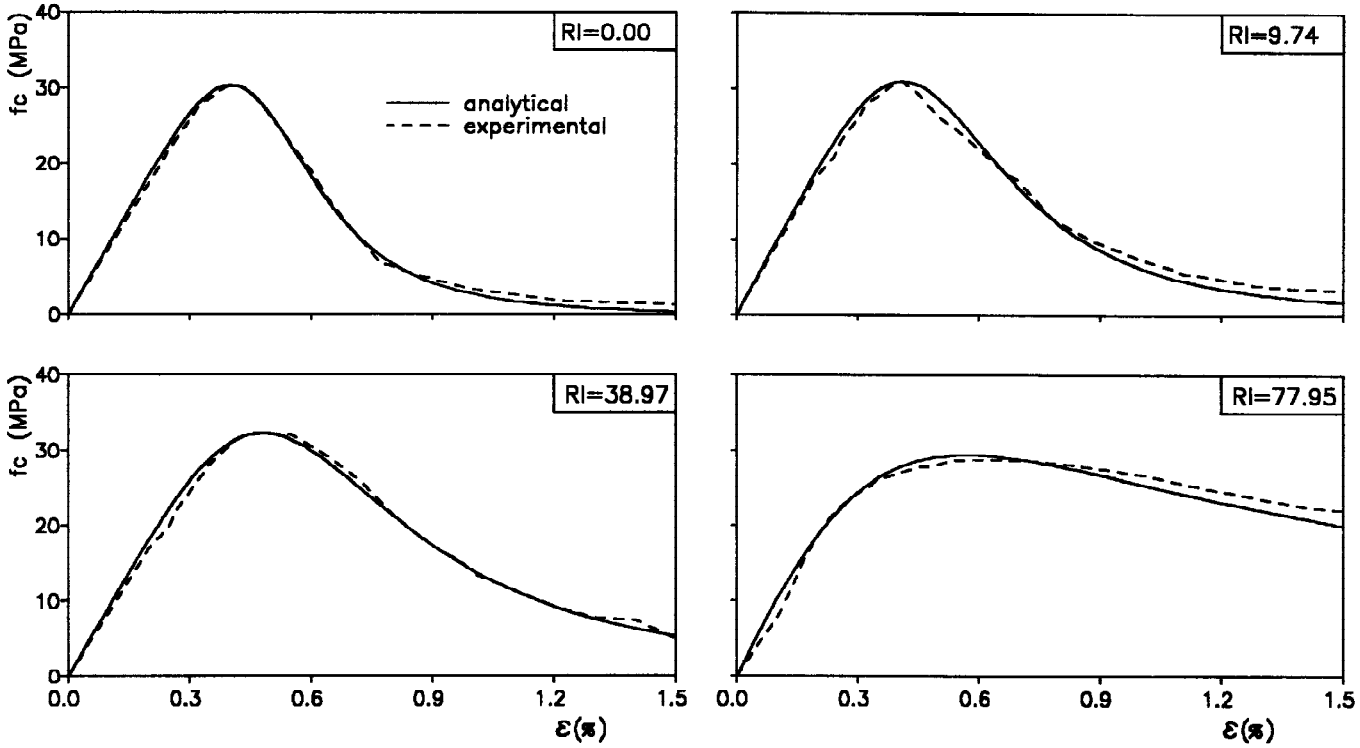

Fig. 1 Experimental and analytical f_c-ε curves of CFRC, varying with RI

The average experimental curves and the analytical curves in each diagram are plotted. The expression for the stress-strain relationship under uniaxial compression is represented by the following equation (Zingone *et.al*,1995):

$$f_c = f_c' \frac{\beta \frac{\varepsilon}{\varepsilon_o}}{\beta - 1 + \left(\frac{\varepsilon}{\varepsilon_o}\right)^{\beta}} \tag{1}$$

where f_c', ε_o are the experimental peak stress and the corresponding strain value. The parameter β, varying with the reinforced index RI, depends on the shape of the stress-strain diagram. For RI equal to 0, 9.74, and 38.97, β can be represented by the following equation:

$$\beta = \beta_0 - 0.5 \cdot (RI)^{\alpha} \tag{2}$$

where α=0.35 and β_0=5.5. If RI=77.95, corresponding to a fraction fibre-volume of 3.04% (high value related to good concrete workability), eq. (2) is still used assuming β=1.95. In Fig. 2 are plotted similar curves of Fig. 1, regarding concrete cylinders with and without fibres confined by steel spirals. In these cases too the stress-strain relationship can be represented by (2) and (3) where β_0 =4.1 and α=0.45 for RI equal to 0, 9.74 and 38.97; if RI=77.95, β=1.45 is assumed.

Comparing the curves in Fig. 2 it can be observed that the confinement exerted by the spiral is added to the fibre's confinement, and if RI increases the fibre's confinement prevails over the spiral's confinement. The analytical stress-strain relationships proposed take the experimental observations into account. The value of β, in the cases of CFRC and CFRC with steel spiral, depends on the shape of the stress-strain diagram, particularly in the descending branch of the curves (if the values of RI increase the descending branch of the curves becomes flatter).

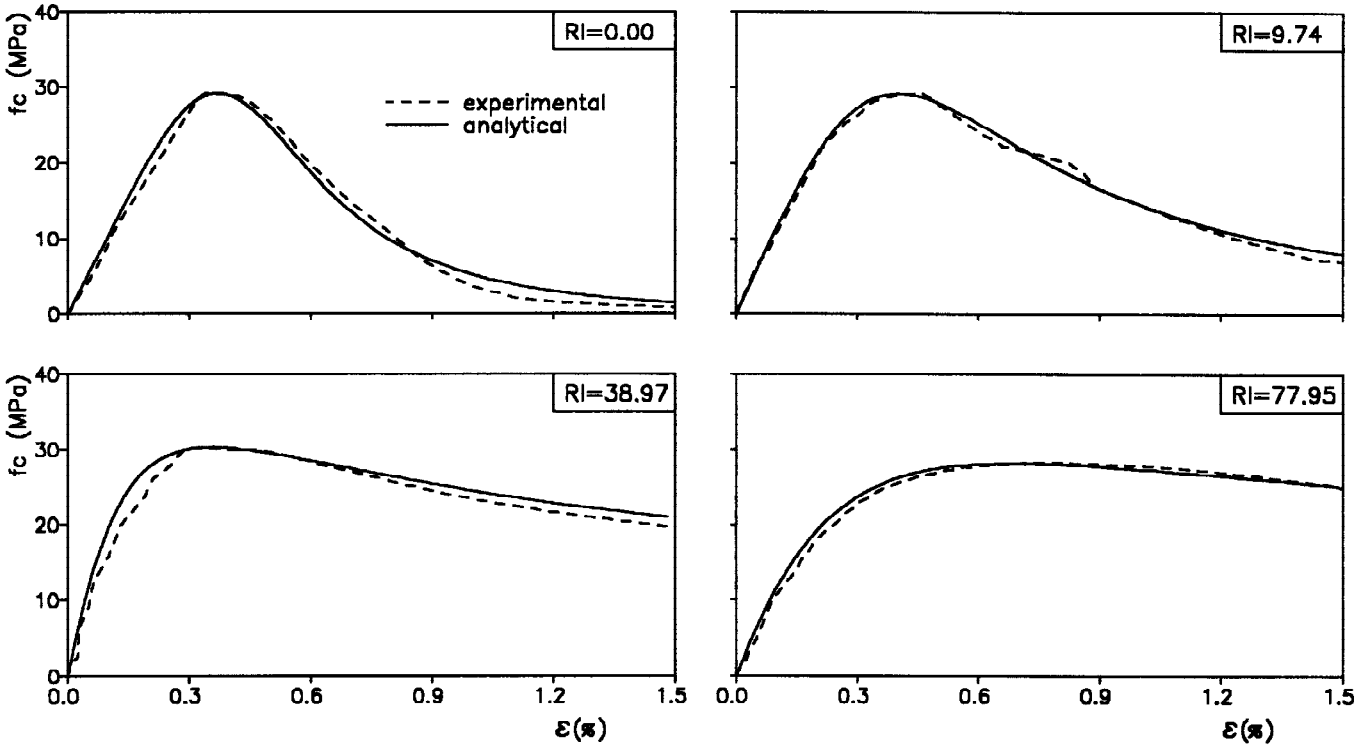

Fig. 2 Experimental and analytical f_c-ε curves of CRFC with spiral, varying with RI

The analytical stress-strain relationship proposed perfectly fit in with the experimental results. The curves are limited to the strain value of 1.5% ; higher values, are not very significant in practical applications.

MONOTONIC TENSILE LOADING

A series of cylindrical specimens under monotonic tensile loading were tested. Indirect tensile (split-cylinder) tests were carried out. The same procedures were used as for the compressive tests (testing machine, strain rate, etc.). In Fig. 3 the experimental results for cylindrical concrete with and without fibres specimens are plotted. The displacement value in abscissa represents the platen-to-platen distance. In each curve are plotted the average experimental results varying with the percentage volume of fibres.

It can be observed that an increase in fibre percentage produce: -an increase in the first-cracking load; -the rise of post-cracking resistance (absent in plain concrete); -an increase in post-cracking load. The values of peak and of post-cracking tensile resistance of CFRC varying with the reinforced index, are shown in Table 1.

Table 1. Peak and post-cracking tensile stresses

RI	Peak stress (*MPa*)	Post-cracking stress (*MPa*)
0.00	3.63	0.00
9.74	4.19	1.95
38.97	4.27	2.45
77.95	5.15	3.25

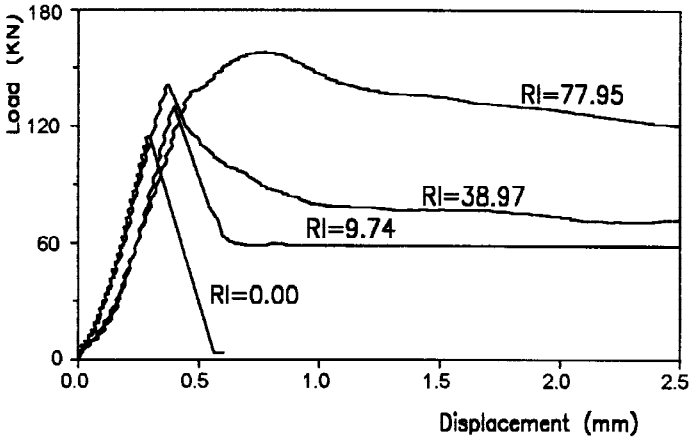

Fig. 3 Experimental results of indirect tensile tests varying with RI

MODELLING OF STRESS-STRAIN CURVE FOR CYCLIC LOADING

Cyclic tests in compression were carried out using the same criterion as for the monotonic tests, for both the unloading and reloading phases. In all tests, the stress-strain curve presents an envelope having the same shape as the monotonic law; therefore it can be expressed analytically by (1).

For the sake of brevity, in Fig. 4 the results of only two tests carried out using specimens with RI=38.97, either in the absence or in the presence of confinement transverse reinforcement, are shown; the value of the parameter β, which fits with to the experimental curve, is 2.8 in the case of Fig. 4 *a*) and 2.35 in the case of Fig. 4 *b*). The cycles for the unloading branch, modelled as in Mander *et.al.*,1988, have the following expression:

$$f_c = f_{un} - \frac{f_{un} \cdot x \cdot r}{r - 1 + x^r} \tag{3}$$

in which

$$x = \frac{\varepsilon - \varepsilon_{un}}{\varepsilon_{pl} - \varepsilon_{un}}; \qquad r = \frac{\frac{f_{un}}{f_c'} \cdot \sqrt{\frac{\varepsilon_o}{\varepsilon_{un}}} \cdot E_c}{\frac{f_{un}}{f_c'} \cdot \sqrt{\frac{\varepsilon_o}{\varepsilon_{un}}} \cdot E_c - \frac{f_{un}}{\varepsilon_{un} - \varepsilon_{pl}}} \tag{4}$$

$$\varepsilon_{pl} = \varepsilon_{un} - \frac{\left(1 + \frac{0.09}{\varepsilon_o} \cdot \sqrt{\varepsilon_{un} \cdot \varepsilon_o}\right) \cdot \varepsilon_{un} \cdot f_{un}}{f_{un} + E_c \cdot \varepsilon_{un} \cdot \frac{0.09}{\varepsilon_o} \sqrt{\varepsilon_{un} \cdot \varepsilon_o}} \qquad E_c = \frac{f_c'}{\varepsilon_o} \cdot \frac{\beta}{\beta - 1} \tag{5}$$

where (ε_{un}, f_{un}) are the coordinates of the unloading point, ε_{pl} the plastic strain and E_c the tangent modulus of elasticity of the concrete. The reloading branch starting from the point of the coordinates (ε_{ro}, f_{ro}) is modelled by a linear law having the following equation:

$$f_c = f_{ro} + \frac{f_{ro} - f_{re}}{\varepsilon_{ro} - \varepsilon_{re}}(\varepsilon - \varepsilon_{ro}) \tag{6}$$

in which (ε_{re}, f_{re}) are the coordinates of the point of intersection between the straight line and the envelope curve; the strain ε_{re} is expressed by

$$\varepsilon_{re} = \varepsilon_{un} + \frac{f_{un} - f_{new}}{3 \cdot \frac{f_{ro} - f_{new}}{\varepsilon_{ro} - \varepsilon_{un}}} \tag{7}$$

with

$$f_{new} = 0.92 \cdot f_{un} + 0.08 \cdot f_{ro} \tag{8}$$

The parabolic transition curve between the linear relation and the envelope curve, as in Mander *et al.*, 1988, is here neglected in order to simplify the calculations. The modelling described is in good agreement with experimental results as shown in Fig. 4.

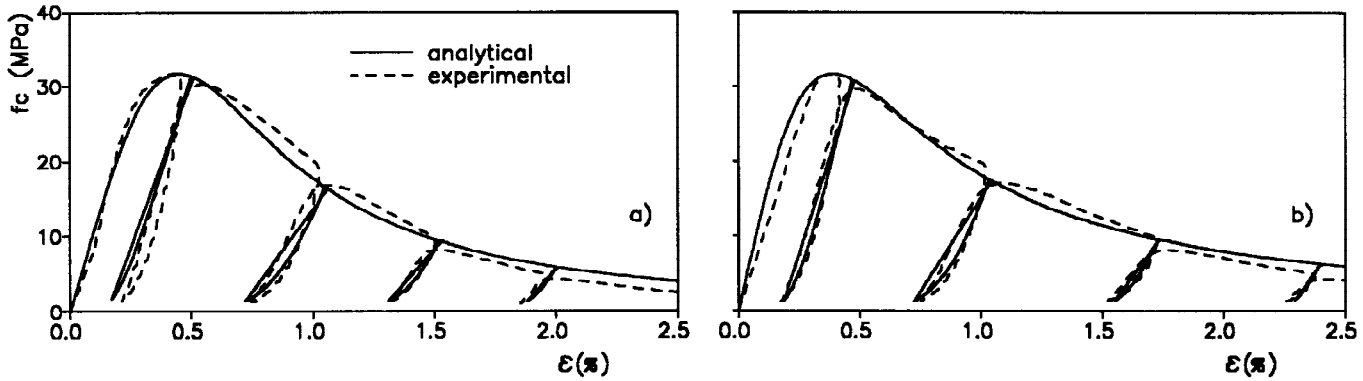

Fig. 4 Experimental and analytical cyclic f_c-ε curve for RI=38.97;
a) CFRC; *b*) CFRC with spiral reinforcement

FLEXURAL CYCLIC BEHAVIOUR

In order to point out the advantages due to the presence of the fibres and to verify the increase in the dissipative capacity of the sections in which the plastic hinges occur, the cyclic moment-curvature diagrams are deduced. These refer to a rectangular cross-section, with equal top and bottom reinforcement, subjected to bending moment combined with an axial load that is assumed to be constant. The CFRC is modelled as described in the above section; the ultimate strain, considered constant in RI, is assumed as the strain at the stress level of 20 percent f_c' on the decreasing branch of the envelope stress-strain curve for RI=0. The steel is modelled as the Goldberg and Richard modified (Giuffrè and Pinto, 1970).

Fig. 5 shows, for two normal force levels, the cycles in terms of $M/(bh^2)$-φh, M being the bending moment evaluated with respect to the centroid of the cross-section; φ is the curvature; b and h the base section and the distance from the top of the section to the centroid of the bottom steel.

In order to evaluate the increase in flexural ductility and dissipative capacity, due to the presence of the fibre in the concrete, diagrams referring to the case in which the confinement due to the transversal reinforcing is negligible with respect to that due to the fibre, are deduced. Therefore, the analytical curves in Fig. 1 are utilised as the envelope of the f_c-ε cyclic law of the CFRC.

The approach adopted is to divide the CFRC section into a number of discrete elements, each of them having the width of the section (Park *et al.*,1972). An iterative technique is used to calculate points on the moment-curvature curve; precisely the strain value ε_c in the top of the CFRC element is adjusted by a fixed amount and for each value of ε_c the neutral axis depth is evaluated iteratively, checking the translational equilibrium equation, then the corresponding bending moment is evaluated by the rotational equilibrium.

The following data are assumed: c/h=0.05, c being the cover; ε_{cu}=0.0082 the ultimate strain of the CFRC; μ= $\mu'=A_s/(bh)$=1%, $A_s=A'_S$ being the longitudinal steel in tension (or in compression); E_s=206010 *MPa* the Young's modulus of the steel; f_{yk}=375 *MPa* is the yielding stress of the steel. In Table 2 the increases in flexural ductility and dissipative capacity with variation in RI are listed; these increases are evaluated with respect to the case of RI=0, and the relative quantities are indicated with the subscript $(\ )_0$. The symbols in Table 2 have the following significance:φ_u= ultimate curvature value corresponding to the ε_{cu} value; φ_y= curvature value corresponding to the first yielding of the steel; D= area included in the cycle.

By increasing the reinforced index RI, it can be observed that: *a*) for the cases examined the flexural ductility can increase up to 30 ÷ 40 percent with respect to the one obtained in the case of RI=0; *b*) the energy dissipation becomes very marked in the case of RI equal to 38.97 and 77.95 for N/(bh)=10 *MPa* being 1.47 times the one corresponding to RI=0.

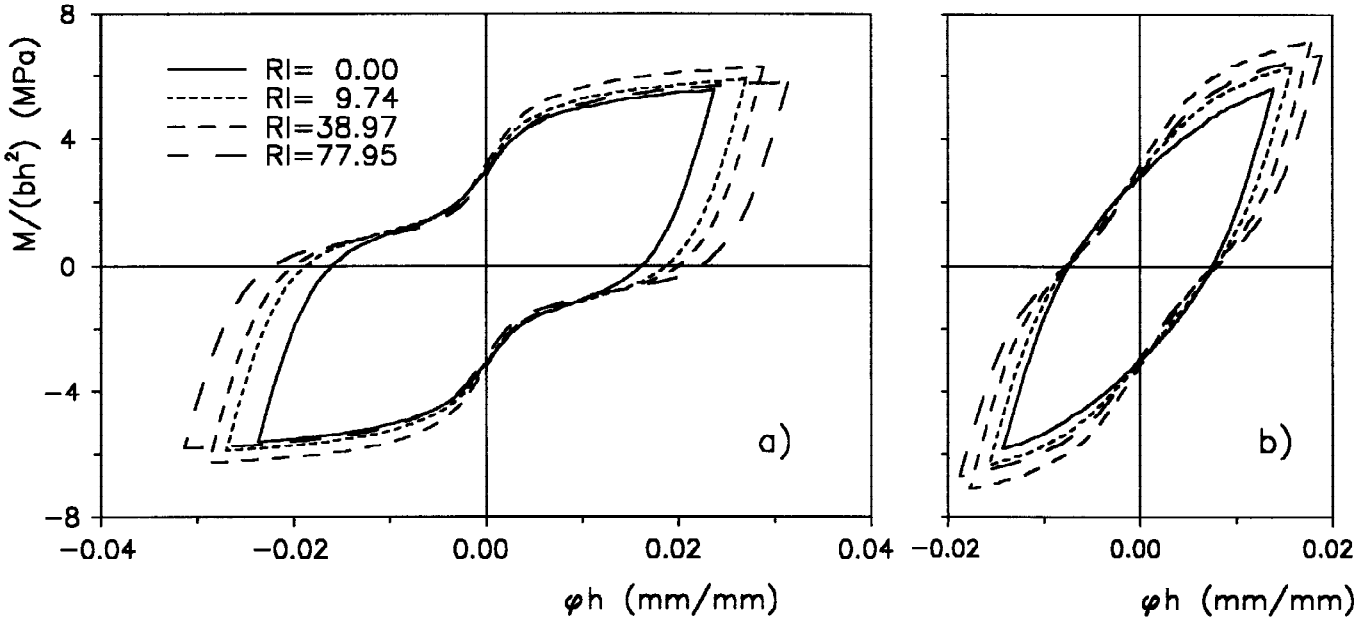

Fig. 5 M/(bh^2)-φh curves with variation in RI: *a*) N/(bh)=6 *MPa*; *b*) N/(bh)=10 *MPa*

Table 2. Flexural ductility and dissipative capacity with variation in RI

		RI=9.74	RI=38.97	RI=77.95
N/bh=6 *MPa*	$\varphi_u/\varphi_y/(\varphi_u/\varphi_y)_o$	1.14	1.20	1.32
	D/D_o	1.20	1.36	1.37
N/bh=10 *MPa*	$\varphi_u/\varphi_y/(\varphi_u/\varphi_y)_o$	1.13	1.27	1.36
	D/D_o	1.19	1.47	1.47

REFERENCES

Bentur, A. and S. Mindess (1990). Fiber reinforced cementitious composities. *Elsevier Science Publishers Ltd.*, New York.

Filiatrault, A., K. Ladicani and B. Massicotte (1994). Seismic performance of code-designed fiber reinforced concrete joints. *Aci Structural Journal*, 91 (5), 564-571.

Giuffrè, A. and P.E. Pinto (1970). Il comportamento del cemento armato per sollecitazioni cicliche di forte intensità. *Giornale del Genio Civile*, 5, 391-408.

Jiuru, T., H. Chaobin , Y. Kaijian and Y. Yongcheng (1992). Seismic behaviour and shear strength of framed joint using steel-fiber reinforced concrete. *Journal of Structural Engineering*, 118 (2), 341-358.

Katzensteiner, B., S. Mindess, A. Filiatrault and N. Banthia (1994). Dynamic tests of steel-fiber reinforced concrete frames. *Concrete International* , 16 (9), 57-60.

Mander, J.B., M.J.N. Priestley and R. Park (1988). Theoretical stress-strain model for confined concrete. *Journal of Structural Engineering*, 114 (8), 1804-1826.

Olariu, I., A.M. Ioani and N. Poienar. (1988). Steel fiber reinforced ductile joints. *Proceeding of Ninth World Conference on Earthquake Engineering*, Tokyo-Kyoto, Japan, 4, 657-662.

Park, R., D.C. Kent and R.A. Sampson (1972). Reinforced concrete members with cyclic loading. *Journal of Structural Division ASCE*, 98 (ST7), 1341-1360.

Zingone, G., L. La Mendola and G. Campione (1995). Resistenza e duttilità di elementi in c.a. rinforzati con fibre di carbonio. *Atti del 7° Convegno Nazionale "L'Ingegneria Sismica in Italia"*, 1, 259-268.